Kinetic and Mechanistic Characterization of an Efficient Hydrolytic Antibody: Evidence for the Formation of an Acyl Intermediate

Jincan Guo, Wei Huang, and Thomas S. Scanlan*

Contribution from the Department of Pharmaceutical Chemistry, University of California at San Francisco, San Francisco, California 94143-0446

Received December 20, 1993®

Abstract: In this paper we report the generation and mechanistic characterization of an unusually active catalytic antibody raised to a phosphonate transition-state analog of norleucine. The antibody (17E8) catalyzes the hydrolysis of both norleucine and methionine phenyl esters and is specific for enantiomers that possess the natural *S* configuration (L) at the α-carbon. The antibody shows side-chain selectivity (k_{cat}/K_M) for norleucine over methionine phenyl esters and also shows selectivity for amino acid ester substrates bearing a formyl substituent at the α-amino position. The antibody-catalyzed hydrolysis of all the ester substrates exhibits a bell-shaped pH-rate profile that is consistent with a mechanistic scheme featuring two ionizable active site residues that mediate catalysis. The calculated pK_a values for these two residues are 8.9 and 10.1, and in the most catalytically active state of the antibody, the pK_a 8.9 residue is deprotonated and the pK_a 10.1 residue is protonated. In the presence of hydroxylamine, partitioning between hydrolysis and hydroxaminolysis is observed, indicating that a covalent acyl intermediate is formed in the antibody-catalyzed reaction. The hydroxaminolysis:hydrolysis product ratio increases with increasing hydroxylamine concentration, while the overall reaction velocity (as measured by phenol release) is unaffected by increasing hydroxylamine concentration. These data support a mechanism involving a covalent acyl intermediate where formation of the intermediate is the rate-determining step in the antibody-catalyzed hydrolysis reaction.

Introduction

Transition-state stabilization has been the most important and successful guiding principle for generating antibodies with enzyme-like properties. The first catalytic antibodies to be generated and characterized were specific for phosphonate and phosphate compounds which are transition-state analogs for ester and carbonate hydrolysis.[1,2] These antibodies catalyze the hydrolysis of esters and carbonates with saturation kinetics that are characteristic of enzyme catalysis. Since these initial discoveries, more than 70 catalytic antibodies have been generated using antigenic compounds (haptens) designed to mimic the stereoelectronic properties of the transition-state for the reaction of interest.[3] Although this strategy has proven to be reliable for obtaining antibodies with catalytic properties, the catalytic activity of the antibodies produced by this method is often lower than natural enzymes that catalyze analogous reactions.

Hydrolytic enzymes such as proteases are among the most efficient enzymes known, as evidenced by high turnover numbers (k_{cat}) and large rate accelerations (k_{cat}/k_{uncat}).[4] The efficiency of these natural catalysts does not arise solely from transition-state stabilization, because the active sites of hydrolytic enzymes also contain cofactors and/or side-chain functional groups that accelerate hydrolysis through nucleophilic, electrophilic, and general acid/base catalysis. It is therefore likely that additional active site chemistry in combination with transition-state stabilization will be required for hydrolytic antibodies to reach the activity levels of hydrolytic enzymes. The strategy of hapten charge complementarity has been used to elicit general acid/base active site residues in hydrolytic antibodies.[5,6] Interestingly, there have been a few reports of hydrolytic antibodies raised to phosphonate and phosphonamidate transition-state analog haptens that appear to possess active site chemistry in addition to that which is responsible for transition-state stabilization.[7-9]

In this paper we report the generation and characterization of an unusually active catalytic antibody that mediates the hydrolysis of unactivated amino acid phenyl esters. The antibody-catalyzed hydrolysis reaction is enantioselective for *S* amino acid esters (natural configuration), has a bell-shaped pH-rate dependence, and mediates hydrolysis through the formation of a covalent acyl intermediate. Although the antibody was raised to a simple phosphonate transition-state analog, it exhibits catalytic properties that suggest a more complex mechanism of action similar to that of the serine protease family of hydrolytic enzymes.

Experimental Section

Synthesis. General Methods and Reagents. Reactions requiring anhydrous conditions were carried out in flame-dried glassware under an atmosphere of nitrogen. Anhydrous solvents were purchased from Aldrich. Chromatography solvents were purchased from Fisher Corp. and were used as received. Reagents were purchased from Sigma or Aldrich and used as received unless noted otherwise. *N*-formyl-L-norleucine was purchased from Bachem Bioscience Inc. Reactions were monitored by thin-layer chromatography (TLC) and HPLC. ^{1}H NMR spectra were recorded on a General Electric 300-MHz instrument. ^{1}H NMR samples were prepared in 5-mm tubes, and chemical shifts were reported in parts per million (δ) downfield relative to an internal standard of tetramethylsilane (0.00 ppm). Mass spectra were recorded on Kratos MS 50 and VG 70 mass spectrometers. Flash chromatography was performed with

* Author to whom correspondence should be addressed.
® Abstract published in *Advance ACS Abstracts*, June 15, 1994.

(1) Pollack, S. J.; Jacobs, J. W.; Schultz, P. G. *Science* **1986**, *234*, 1570–3.
(2) Tramontano, A.; Janda, K. D.; Lerner, R. A. *Science* **1986**, *234*, 1566–70.
(3) Lerner, R. A.; Benkovic, S. J.; Schultz, P. G. *Science* **1991**, *252*, 659–67.
(4) Fersht, A. *Enzyme Structure and Mechanism*; Freeman: New York, 1985, pp 405–426.
(5) Janda, K. D.; Weinhouse, M.; Schloeder, D. M.; Lerner, R. A.; Benkovic, S. J. *J. Am. Chem. Soc.* **1990**, *112*, 1274–5.
(6) Janda, K. D.; Weinhouse, M. I.; Danon, T.; Pacelli, K. A.; Schloeder, D. M. *J. Am. Chem. Soc.* **1991**, *113*, 5427–34.
(7) (a) Benkovic, S. J.; Adams, J. A.; Borders, C. L., Jr.; Janda, K. M.; Lerner, R. A. *Science* **1990**, *250*, 1135–9. (b) Wirsching, P.; Ashley, J. A.; Benkovic, S. J.; Janda, K. D.; Lerner, R. A. *Science* **1991**, *252*, 680–5.
(8) Martin, M. T.; Napper, A. D.; Schultz, P. G.; Rees, A. R. *Biochemistry* **1991**, *30*, 9757–61.
(9) Tramontano, A.; Ammann, A. A.; Lerner, R. A. *J. Am. Chem. Soc.* **1988**, *110*, 2282–6.

0002-7863/94/1516-6062$04.50/0

Merck silica gel 60 (230–400 mesh). Ion exchange resins were purchased from Bio-Rad and were converted to the necessary ion form according to the manufacturer's recommendations.

Diphenyl [1-(1-*N*-Benzyloxycarbonylamino)pentyl]phosphonate, 6. A mixture of triphenyl phosphite (30.0 g, 0.097 mol), *n*-pentanal (26.0 g, 1.5 equiv, freshly distilled), benzyl carbarmate (62.2 g, 1.0 equiv), and glacial acetic acid (30 mL) was stirred in a water bath at room temperature for 1 h until the exothermic reaction subsided. The water bath was removed, and the reaction was heated to 50 °C for 2 h. Acetic acid and volatile by-products were removed by rotary evaporation to give an oily residue, which was dissolved in 360 mL of methanol and left at 4 °C overnight. Phosphonate **6** was collected by filtration and recrystallized from chloroform–methanol (37.0 g, 40%). ^{1}H NMR ($DCCl_3$): 7.20-7.40 (m, 15H), 5.25 (2H, m), 4.40–4.55 (1H, m), 2.30–2.50 (1H, br s), 2.00–2.20 (2H, m), 1.30–1.70 (6H, m), 0.90 (3H, t, J = 6.2 Hz). LSIMS-MS m/z (rel int): 454.1 ($M + H^+$) (100), 360 (15), 325.0 (25), 270.0 (15), 220.1 (23), 176.1 (82). High-resolution MS (EI): calcd for $C_{19}H_{23}NO_4P$ (M^+ – PhO), 360.1369; found, 360.1365.

Diphenyl [1-(1-Amino)pentyl]phosphonate Hydrochloride, 7. Phosphonate **6** (15.0 g, 0.033 mol) was dissolved in 10 mL of hydrogen bromide (30% in acetic acid), and the mixture was stirred for 1 h at room temperature. Water (400 mL) and diethyl ether (400 mL) were added to the reaction mixture, and the resulting two-phase suspension was stirred at room temperature for 10 min. Sodium hydroxide solution (5 M) was added to adjust the pH in the aqueous phase to 9.0. The organic phase was then separated and washed two times with water (100 mL). Aminophosphonate **7** was precipitated as the hydrochloride salt by addition of 20 mL of aqueous HCl (4 M). The product was filtered and dried to yield 11.0 g (93.4%) of **7** as a white powder. ^{1}H NMR (DMSO-d_6): 9.05 (3H, br s, NH_3^+), 7.25–7.45 (10H, m), 4.10 (1H, m), 2.00 (2H, m), 1.55 (2H, m), 1.40 (2H, m), 0.80 (3H, t, J = 6.1 Hz). LSIMS-MS m/z (rel int): 320.1 ($M - Cl^-$) (100).

Diphenyl [1-(1-*N*-Succinylamino)pentyl]phosphonate, 8. To a solution of **7** (4.8 g 15.0 mmol) in 20 mL of pyridine was added succinic anhydride (4.8 g, 3 equiv) and the reaction mixture was stirred at room temperature for 18 h. HPLC analysis indicated the completion of the reaction. Water (20 mL) was added to the reaction mixture, and stirring was continued for an additional 2 h. Ethyl acetate (200 mL) and concentrated HCl (40 mL) were then added to the reaction mixture. The ethyl acetate phase was collected and washed with 1.0 M HCl (50 mL × 4), water (50 mL × 2), and saturated $NaHCO_3$ (50 mL × 2). The ethyl acetate was evaporated, and the crude product was purified by flash chromatography eluting with 1% acetic acid in ethyl acetate, providing 2.8 g (45%) of **8** as a white powder. ^{1}H NMR ($DCCl_3$): 7.05–7.50 (10H, m), 4.75–4.95 (1H, m), 2.14–2.70 (4H, m), 1.86–2.00 (1H, m), 1.62–1.80 (1H, m), 1.18–1.50 (4H, m), 0.85 (3H, t, J = 5.5 Hz). LSIMS-MS m/z (rel int): 420.2 ($M + H^+$) (35), 344.2 (50), 326.2 (25), 268.1 (60), 250.1 (100), 186.1 (30). High-resolution MS (EI): calcd for $C_{15}H_{19}NO_4P$ (M^+ – PhO, H_2O), 308.1061; found, 308.1052.

Phenyl [1-(1-*N*-Succinylamino)pentyl]phosphonate, 5. To a flask containing **8** (2.5 g, 6.0 mmol) was added 40 mL of 2 N NaOH, and the reaction mixture was stirred at room temperature for 20 h. The mixture was then loaded onto a cation-exchange column (Dowex, 100 mesh, 2.5 × 10 cm, H^+ form) and eluted with water. The eluent was collected, extracted three times with chloroform (50 mL each), and lyophilized. The lyophilized powder was dissolved in 3 mL of water and purified by HPLC (Dynamax C_{18}, 10-μm pack, 2.0 × 10 cm). A flow rate of 10 mL/min was used with a linear gradient of 10% B to 80% B over 20 min (A, 0.1% trifluoroacetic acid in water; B, acetonitrile). Fractions containing the desired product were pooled and lyophilized. The residue was dissolved in 3 mL of water, and the pH was adjusted to pH 6.0 with 1 N NaOH. The solution was lyophilized again, providing 800 mg (33%) of **5** as the sodium salt. ^{1}H NMR (D_2O): 7.34 (2H, t, J = 7.9 Hz), 7.16 (3H, m), 4.18 (1H, m), 2.50 (4H, m), 1.86 (2H, m), 1.62 (2H, m), 1.23–1.39 (4H, m), 0.86 (3H, t, J = 6.1 Hz). LSIMS-MS m/z (rel int): 386 ($M - H^+$) (35), 364 ($M - Na^+$) (100), 342 (25), 183 (30). The product was converted to the lithium salt by loading an aqueous solution of **5** onto a cation-exchange column (Dowex, 100 mesh, 1.5 × 10 cm, Li^+ form) and eluting with water. The eluent was collected and lyophilized, affording the lithium salt of **5** as a white powder.

Preparation of KLH-5 and BSA-5 Protein Conjugates. BSA-5. Hapten **5** (18.0 mg, 0.049 mmol) and bovine serum albumin (BSA) (30 mg) were dissolved in 1.0 mL of water. The pH of the solution was adjusted to 6.0 with 2.0 N HCl, and then 1-(3-(dimethylamino)propyl)-3-ethylcarbodiimide hydrochloride (EDC) (7.8 mg, 0.049 mmol) was added. After stirring at room temperature for 1 h, a second equivalent of EDC was added, and the reaction was stirred at 4 °C for 18 h. The reaction mixture was extensively dialyzed against PBS (50 mM $NaHPO_4$, 150 mM NaCl, pH 7.2), affording 12.6 mg of **BSA-5** conjugate.

KLH-5. To a solution of KLH (20 mg) and **5** (43 mg, 0.12 mmol) in 1.0 mL of water (adjusted to pH 6.5 with 2 N HCl) was added EDC (18.0 mg, 0.12 mmol), and the mixture was stirred at room temperature. One hour later, an additional equivalent of EDC (18.0 mg) was added, and the reaction was left at 4 °C overnight. The reaction mixture was then dialyzed against PBS and filtered (0.45 μm), giving a PBS solution containing 18 mg of **KLH-5**.

Synthesis of Amino Acid Ester Substrates 1–4. Substrates **1–4** were prepared by esterifying *N*-formyl and *N*-acetyl norleucine and methionine with phenol using dicyclohexylcarbodiimide (DCC) as the coupling reagent. The general procedure was as follows: to an ice-cold solution of amino acid (**1–4**) (10 mmol) and phenol (20 mmol) in 20 mL of dichloromethane was added 20 mmol DCC. The reaction was stirred in an ice bath for 1 h and then at room temperature for 3 h. The resulting suspensions were filtered, and the filtrate was evaporated to dryness. The crude esters were purified by flash chromatography, eluting with 500 mL of 20% ethyl acetate–hexanes followed with 700 mL of 50% ethyl acetate–hexanes for the preparation of **1** and **2** or with 700 mL of ethyl acetate for the preparation of **3** and **4**.

Ac-norleuOPh, 1. Yield: 90.3%. ^{1}H NMR ($DCCl_3$): 7.38 (2H, t, J = 8.7 Hz), 7.22 (1H, t, J = 8.7 Hz), 7.06 (2H, d, J = 9.0 Hz), 6.26 (1H, br d, J = 7.9 Hz), 4.84 (1H, m), 2.04 (3H, s), 2.00 (1H, m), 1.83 (1H, m), 1.40 (4H, m), 0.92 (3H, t, J = 7.2 Hz). LSIMS-MS m/z (rel int): 250.1 ($M + H^+$) (100), 208.1 (10), 156.1 (70), 128.2 (95).

For-norleuOPh, 2. Yield: 81.0%. ^{1}H NMR ($DCCl_3$): 7.42 (2H, t, J = 9.0 Hz), 7.24 (1H, t, J = 9.0 Hz), 7.10 (2H, d, J = 9.0), 6.38 (1H, br d, J = 7.2 Hz), 4.96 (1H, m), 2.10 (1H, m), 1.95 (1H, m), 1.25–1.46 (4H, m), 0.92 (3H, t, J = 7.1). LSIMS-MS m/z (rel int): 236.2 ($M + H^+$) (100), 142.2 (53), 114.2 (35).

Ac-metOPh, 3. Yield: 75.7%. ^{1}H NMR ($DCCl_3$): 7.40 (2H, t, J = 10), 7.23 (1H, t, J = 10.2 Hz), 7.15 (2H, d, J = 10.2 Hz), 6.38 (1H, d, J = 9.0 Hz), 4.98 (1H, m), 2.62 (2H, t, J = 6 Hz), 2.25–2.40 (1H, m), 2.18 (1H, m), 2.16 (3H, s), 2.06 (3H, s). LSIMS-MS m/z (rel int): 268.1 ($M + H^+$) (100), 220.1 (22), 174.1 (78).

For-metOPh, 4. Yield: 74% yield. ^{1}H NMR ($DCCl_3$): 8.24 (1H, s), 7.42 (2H, t, J = 9.2 Hz), 7.24 (1H, t, J = 9.2 Hz), 7.16 (2H, d, J = 9.4 Hz), 6.60 (1H, br s), 5.06 (1H, m), 2.63 (2H, t, J = 6.2 Hz), 2.38–2.42 (1H, m), 2.18–2.22 (1H, m), 2.17 (3H, s). LSIMS-MS m/z (rel int): 254.1 ($M + H^+$) (100), 220.1 (22), 174.1 (78).

Antibody Production. Balb/c mice (6-week old females) were immunized with the KLH conjugate of hapten **5** (KLH-**5**) according to the following schedule: day 1, 200 μg of KLH-**5** + complete Freund's adjuvant, intraperitoneal injection; day 14, 200 μg of KLH-**5** + incomplete Freund's adjuvant, intraperotoneal injection; day 17, serum-titer check (ELISA using bovine serum albumin-**5** conjugate); day 47, hyperimmunization, 50 μg of KLH-**5** in saline, intravenous injection. Four days after hyperimmunization, spleenectomy was performed on one mouse and the resulting spleenocytes were fused (polyethylene glycol) with 10^8 sp2/0 myelomas and plated into 40 96-well culture plates in HAT selection media (RPMI, 20% fetal bovine serum, 10% Origen Hybridoma Factor (IGEN), HAT, penicillin/streptomycin). Hybridoma growth wells were first screened for hapten affinity with a standard ELISA format using the bovine serum albumin conjugate of hapten **5** (BSA-**5**). A goat antimouse IgG alkaline phosphatase conjugate was used as a secondary antibody. Positives wells from this screen were then analyzed in a secondary screen for the ability to bind soluble hapten **5**. This secondary screen was conducted in a hapten-inhibition ELISA format using BSA-**5** and soluble hapten **5**. Positives from this secondary screen were cloned by limiting dilution techniques that resulted in 20 stable monoclonal cell lines.[10] Samples of the monoclonal antibodies were prepared by injecting 2×10^7 hybridoma cells into pristane-primed balb/c mice (10-week old females), the resulting ascites fluid was collected, and monoclonal antibody was purified from ascites fluid by protein-A affinity chromatography.[10] The antibody samples were analyzed for purity using SDS–polyacrylamide gel electrophoresis (SDS-PAGE, 12% acrylamide gels) and visualized with Coomassie blue staining. The antibody samples were dialyzed into PBS buffer (50 mM $NaHPO_4$, 150 mM NaCl, pH 7.2) for activity assays.

Activity Assays. The initial activity screens of the panel of 20 monoclonal antibodies were performed with a continuous spectrophotometric assay using a Uvikon 930 (Kontron Instruments) UV–vis

(10) Harlow, E.; Lane, D. *Antibodies: A Laboratory Manual*; Cold Spring Harbor: Cold Spring Harbor, NY, 1988; p 350.

spectrophotometer with cuvette holders thermostated to 24 °C with a Lauda RM6 temperature control unit. Catalytic activity was measured as a function of phenol release by monitoring increasing absorbance at 270 nm (ϵ = 1500 M^{-1} cm^{-1} for phenol in PBS).[11] The assays were carried out in 0.5-mL cuvettes by adding 20 μL of a 2.5 mM stock solution of racemic substrate **1** to 480 μL of a 6.7 μM PBS solution of each antibody and monitoring increasing absorbance at 270 nm. The background velocity in PBS was also measured in this manner using PBS buffer not containing antibody. Four of the 20 monoclonal antibodies identified from this assay catalyzed the hydrolysis of **1** at a rate above the background reaction.

Enantioselectivity Measurements. We were only able to prepare substrates **1–4** in approximately 50% enantiomeric excess from enantiomerically pure (L or D) formyl or acetyl norleucine or methionine presumably because of oxazalone formation and racemization during phenol coupling (see synthesis section). The enantiomeric excess of substrates **1–4** prepared from enantiomerically pure amino acid starting materials was measured by NMR using the chiral shift reagent Tris-[3-[(heptafluoropropyl)hydroxymethylene]-(+)-camphorato]europium-(III) with the racemic ester substrates **1–4** used as controls. Each of the enantiomerically enriched substrates analyzed in this manner contained approximately 75 mol % (50% ee) of the enantiomer with the same configuration as the L or D amino acid starting material. We were able to use the L and D enantiomerically enriched substrates to determine the enantioselectivity of the 17E8-catalyzed hydrolysis. The analysis was performed by comparing the velocities obtained using racemic substrates **1–4** (1:1, L:D) at a total substrate concentration (L + D) ≤ (1/2)V_{max} with the velocities obtained using the L enantiomerically enriched substrates (3:1, L:D) at the same total substrate concentration. This comparison showed that the velocities obtained using the L-enriched substrates proceeded at a faster rate, which corresponded to the presence of a 50% higher effective substrate concentration, consistent with the 17E8-catalyzed reaction being selective for the L amino acid ester enantiomer.

Kinetic Analysis of 17E8 at pH 8.7. Full steady-state kinetic analysis was performed on antibody 17E8 with the L enantiomerically enriched ester substrates **1–4** using the continuous spectrophotometric assay described above. For the norleucine esters **1** and **2**, substrate concentrations in the range 50 μM to 2.0 mM were used; substrate concentrations between 250 μM and 8.0 mM were used for the methionine esters **3** and **4**. The antibody 17E8 was used at either 0.42 or 0.84 μM concentration in 50 mM Tris–150 mM NaCl, pH 8.7 (TBS-8.7). Reactions were initiated as described above by adding a 25× DMSO stock solution of substrate to the antibody at 24 °C in TBS-8.7 buffer. The background reaction was measured in an analogous manner (TBS-8.7, no antibody), and antibody-catalyzed initial rates were corrected by subtracting the background rate. The K_M and k_{cat} values were determined from double-reciprocal plots ($1/V$ vs $1/[S]$) of the initial rate data. The substrate concentrations were corrected to effective substrate concentrations, taking into account the 50% ee of the L enantiomer (3:1, L:D).

Hapten Inhibition of 17E8 Catalysis. The hapten inhibition experiment was performed by measuring the initial rate of the 17E8-catalyzed hydrolysis of substrate **1** at two fixed concentrations (200 and 500 μM) in the presence of varying concentrations of hapten **5** (0.2, 1.0, and 5.0 μM) in 50 mM Tris–150 mM NaCl, at pH 8.3 (0.56 μM antibody). The inhibition data were analyzed according to the method of Dixon by plotting $1/V$ vs [**5**].[12]

17E8 Fab Preparation. To a solution of 40 mg of 17E8 immunoglobulin in 10 mL of 100 mM $NaHPO_4$ and 4.0 mM EDTA, pH 7.2, was added DTT from a freshly prepared 100 mM stock solution to a final concentration of 1.0 mM. Papain was added (16 μL, 25 mg/mL), and the reaction mixture was incubated at 37 °C for 4 h. The reaction mixture was then filtered (0.45-μm syringe filter) and applied to a 1.5 × 100 cm Sepharose G-50 column. The antibody fragments were eluted from the column with PBS (first protein fraction to elute as monitored by A_{280}), and this eluate was then subjected to protein-A affinity chromatography.[10] The flow-through fractions from the protein-A column containing the 17E8 Fab fragment were pooled, dialyzed against PBS, and concentrated by ammonium sulfate precipitation. The Fab fragment was judged to be >95% homogeneous by SDS-PAGE (with reducing and nonreducing sample buffer) visualized with Coomassie blue staining. The specific activity of the 17E8 Fab was compared to the specific activity of the intact 17E8 immunoglobulin in a side-by-side initial velocity measurement that showed that the Fab fragment had the same specific activity as the intact immunoglobulin.

pH-Rate Dependence of 17E8 Catalysis. The steady-state kinetics of 17E8-catalyzed hydrolysis of substrates **1–4** were analyzed as a function of pH using the same method described above for the pH 8.7 kinetic analysis. The following buffer systems were used in this analysis: 50 mM $NaHPO_4$, 150 mM NaCl, pH 7.2; 50 mM Tris, 150 mM NaCl, pH 7.8, 8.3, and 8.7; 50 mM CHES, 150 mM NaCl, pH 9.0, 9.5, and 10.0; 50 mM CAPS, 150 mM NaCl, pH 10.25 and 10.5. The values of k_{cat} and K_M for each substrate at each pH were obtained from double-reciprocal plots ($1/V$ vs $1/[S]$) of the initial rate data corrected for the background reaction. The k_{cat} values for each substrate were plotted as a function of pH, and the resulting profiles were fit to the equation described in ref 20 using the Kaliedagraph plotting program.

17E8-Catalyzed Preparation of Hydroxamate 9. Ester **1** (154 mg) was added to a solution of 17E8 (25 mg) in 12 mL of 100 mM hydroxylamine–50 mM CHES–150 mM NaCl, pH 9.0. The reaction mixture was stirred for 1 h at room temperature, filtered, and extracted with chloroform. Hydroxamate **9** was purified from the aqueous layer by reverse-phase HPLC (Dynamax C_{18}, 10-μm pack, 2.0 × 10 cm column; solvent A, 0.1% aqueous TFA, solvent B, 0.1% TFA in acetonitrile; flow rate of 10 mL/min). A linear gradient from 10% B to 80% B over 24 min was used (UV detection at 215 nm), and the retention time of hydroxamate **9** was 14.5 min. The fractions containing **9** were lyophilized, providing 54 mg of **9** as a white solid. 1H NMR (D_2O): 0.90 (3H, t, J = 7.0 Hz), 1.30–1.42 (4H, m), 1.73–1.78 (1H, m), 1.84–1.99 (1H, m), 2.06 (3H, s), 4.32 (1H, dd, J = 8.8, 5.0 Hz). High-resolution MS (EI): calcd for $C_8H_{14}NO_2$ (M^+ – NHOH), 156.1030; found, 156.1025.

Hydroxylamine Partitioning Studies. This analysis was performed using a modification of the procedure reported by Bernhard for chymotrypsin.[13] The following stock solutions were freshly prepared prior to the experiments: 25 mM ester **1** in acetonitrile; 17E8 in PBS (2.9 mg/mL); pH 9.5 buffer consisting of 50 mM CHES and 150 mM NaCl, pH 9.5; 500 mM NH_2OH in pH 9.5 buffer; 1.0 M trifluoroacetic acid (TFA) in water; 10% (w/v) $FeCl_3$ in 0.2 M HCl. All solutions except the substrate stock solution were equilibrated to 24.5 °C.

Initial rate measurements were carried out at 24.5 °C by adding 0–30 μL of the hydroxylamine stock solution to a 1.0 mL cuvette followed by 25 μL of the antibody solution. The pH 9.5 buffer was added to a final volume of 480 μL. The substrate **1** stock solution (20 μL) was added to the cuvette, and phenol release was measured at 270 nm to 10% conversion (final [NH_2OH] = 0–30 mM, final [17E8] = 0.91 μM). After the rate measurement was complete, the reaction was immediately quenched by adding 50 μL of TFA solution, and hydroxamic acid quantitation was performed. Quantitation of total product conversion (**9** + **10**) at each hydroxylamine concentration was calculated from the amount of liberated phenol prior to the acid quench. Buffer-catalyzed reaction rates with no added antibody were performed analogously at each hydroxylamine concentration.

Hydroxamic acid quantitation was performed by adding 100 μL of the $FeCl_3$ solution to 500 μL of the quenched reaction mixture and incubating the resulting solution for exactly 5 min at 24.5 °C. The optical density was then measured at 520 nm. The amount of hydroxamic acid product **9** was then calculated from a standard curve prepared using a flanking range of concentrations of authentic **9** with the same procedure. Formation of **9** was observed in the background reaction (with no antibody), although to a lesser extent than reactions carried out in the presence of 17E8. Buffer-catalyzed levels of **9** were determined analogously from reaction mixtures with no added antibody.

Cloning and Sequencing of Antibody Genes. Poly(A)+ mRNA was isolated from 5 × 10^7 17E8 hybridoma cells using the guanidinium thiocyanate method.[14] Synthesis of immunoglobulin Fab cDNA was performed by standard procedures.[15] The light- and heavy-chain Fab genes were amplified through 30 cycles of PCR using the Fab-specific primers designed by Winter *et al.*[16] that included *Not*I and *Nsi*I overhanging restriction sites that allow the amplified material to be cloned into the Fab expression vector pTSS1.[15] The light- and heavy-chain genes were cloned into separate constructs, and nucleotide sequence analysis was performed at the Biomolecular Resource Center (UCSF)

(11) Napper, A. D.; Benkovic, S. J.; Tramontano, A.; Lerner, R. A. *Science* **1987**, *237*, 1041–3.
(12) Dixon, G. *Biochem. J.* **1953**, *55*, 170–5.
(13) Bernhard, S. A.; Coles, W. C.; Nowell, J. F. *J. Am. Chem. Soc.* **1960**, *82*, 3043–50.
(14) Chomczynski, P.; Sacchi, N. *Anal. Biochem.* **1987**, *162*, 156–9.
(15) Lesley, S. A.; Patten, P. A.; Schultz, P. G. *Proc. Natl. Acad. Sci.* **1993**, *90*, 1160–5.
(16) Hoogenboom, H. R.; Griffiths, A. D.; Johnson, K. S.; Chiswell, D. J.; Hudson, P.; Winter, G. *Nucleic Acids Res.* **1991**, *19*, 4133–7.

Scheme 1. Synthesis of Hapten **5**

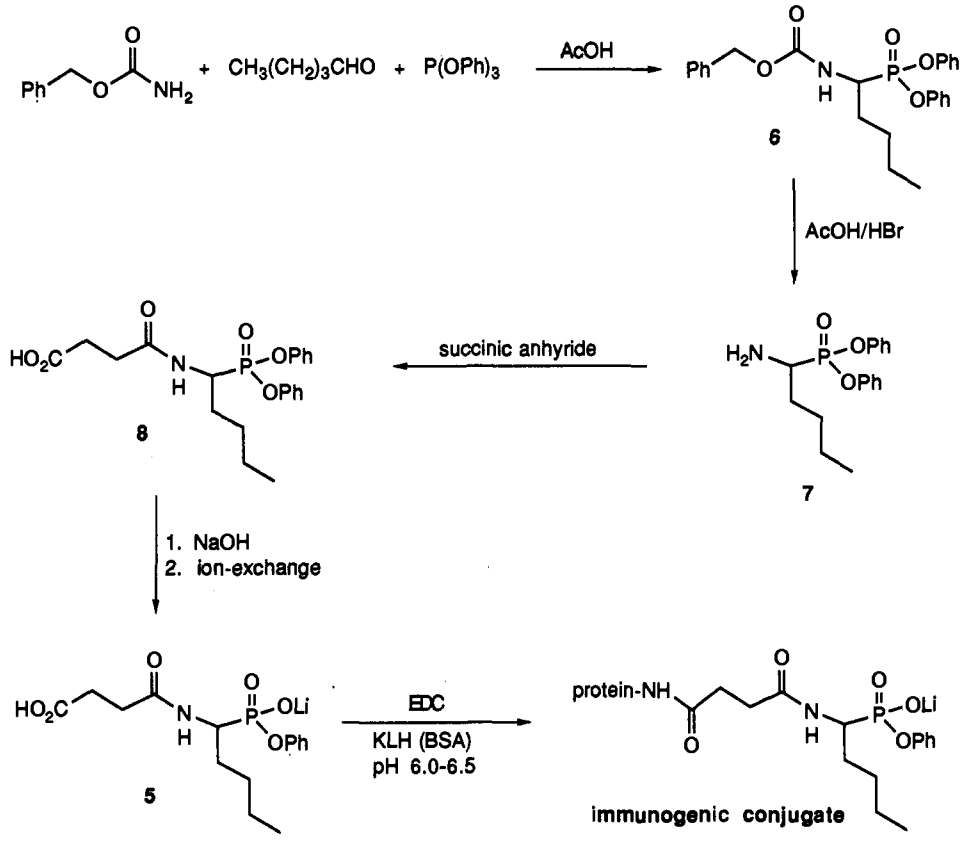

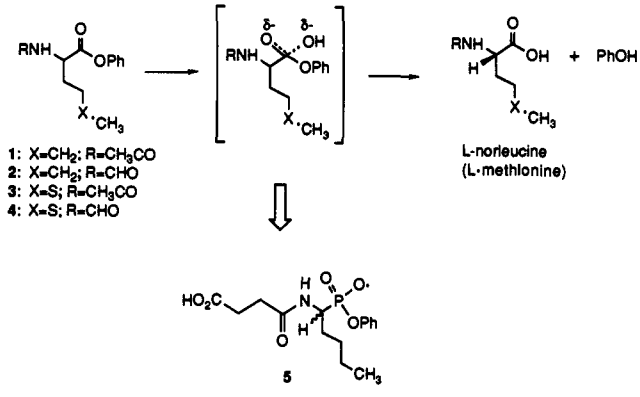

Figure 1. Hapten design for amino acid ester hydrolysis.

by the method of Taq-dye terminator cycle sequencing using an Applied Biosystems 370A instrument.

Results

Hapten Synthesis and Antibody Production. We were interested in obtaining a catalytic antibody capable of hydrolyzing α-amino acid esters because an antibody with this activity would represent a starting point for the development of proteolytic catalysts and could also be used to develop a functional selection for identifying antibody mutants with improved hydrolytic activity.[15,17] The reaction we chose to target was the hydrolysis of methionine phenyl esters (Figure 1). It is now well documented that transition-state mimics such as phosphonate **5** are effective antigens (haptens) for eliciting antibodies capable of catalyzing hydrolysis of the corresponding ester.[3] After incurring synthetic difficulties with methionine phosphonate analogs, we decided to prepare hapten **5** as the norleucine phosphonate analog where the side-chain methionine thioether is replaced by a methylene unit. We viewed this as a conservative substitution on steric and electronic grounds and were interested in quantitating any effect this substitution might have by testing the panel of methionine and norleucine esters **1**–**4** as substrates for antibodies raised to phosphonate **5**.

Hapten **5** was prepared as a racemic mixture in five steps from *n*-pentanal, as described in Scheme 1. Hapten **5** was coupled to the carrier proteins keyhole limpet hemocyanin (KLH) and bovine serum albumin (BSA) using a water-soluble carbodiimide reagent (EDC) to provide the corresponding protein conjugates.[18] The KLH conjugate was used as an antigen, and the BSA conjugate was used in ELISA experiments for measuring serum titer and hapten affinity.

Balb/c mice were immunized with the KLH conjugate of **5**, and hybridomas were prepared from the immunized spleenocytes using standard procedures.[10] Hybridoma supernatants were screened for the presence of antibodies with affinity for the BSA conjugate of hapten **5**, and positives from this primary screen were tested in a secondary screen for the ability to bind hapten **5** free in solution. From this two-step screening procedure we obtained 20 stable hybridoma cell lines that produced antibodies specific for **5**. Samples of monoclonal antibodies were prepared by *in vivo* ascites production and purified from ascites fluid to >95% homogeneity (as judged by SDS-PAGE) by protein-A affinity chromatography.

Activity Assays and Kinetic Analysis. The panel of 20 **5**-specific antibodies were initially screened for the ability to catalyze the hydrolysis of the racemic acetyl norleucine ester **1**. Activity measurements were conducted with a continuous spectrophotometric assay which monitored the appearance of phenol, and product analysis was confirmed by HPLC.[11] Four of the 20 antibodies were found to catalyze the hydrolysis at a rate above the background reaction, and one antibody in particular (clone 17E8) performed catalysis with a large rate acceleration and was characterized in detail.

(17) Tang, Y.; Hicks, J. B.; Hilvert, D. *Proc. Natl. Acad. Sci. U.S.A.* **1991**, *88*, 8784–6.

(18) Erlanger, B. *Methods Enzymol.* **1980**, *70*, 85–103.

Table 1. Kinetic Parameters for 178E8-Catalyzed Ester Hydrolysis at pH 8.7[a]

substrate	k_{cat} (min^{-1})	K_M (μM)	k_{cat}/K_M (M^{-1} min^{-1})	k_{uncat} (min^{-1})	k_{cat}/k_{uncat}
1	49.0 ± 1.7	215 ± 33	2.3×10^5	5.5×10^{-3}	8.9×10^3
2	101.4 ± 0.6	259 ± 2	3.9×10^5	7.9×10^{-3}	1.3×10^4
3	31.1 ± 1.1	1033 ± 12	3.0×10^4	1.7×10^{-2}	1.8×10^3
4	141 ± 16	2270 ± 230	6.2×10^4	1.3×10^{-2}	1.1×10^4

[a] Kinetic constants k_{cat} and K_M were obtained from double-reciprocal plots of initial rate data (described in the Experimental Section). 17E8-catalyzed reactions were conducted in 50 mM Tris–150 mM NaCl at pH 8.7 with 0.5 μM 17E8. The uncatalyzed reaction (k_{uncat}) was measured in this same buffer system without added antibody. The antibody-catalyzed velocities are corrected in that the background velocity is subtracted.

We first examined the enantioselectivity of hydrolysis and found that the enantiomer of **1** which corresponded to the natural *S* configuration (L) functioned as a substrate for 17E8, whereas hydrolysis of the *R* enantiomer (D) was not catalyzed by 17E8 at a rate above the spontaneous background reaction. All *N*-acetyl and *N*-formyl norleucine and methionine esters **1–4** were acceptable substrates for 17E8 with the same L-specific enantioselectivity. Next, we evaluated the kinetic parameters of 17E8 catalysis by measuring initial rates of hydrolysis with varying concentrations of substrate at pH 8.7. The catalysis observed for 17E8 displayed saturation kinetics consistent with Michaelis–Menten enzyme kinetics. The initial rate data were evaluated by double-reciprocal plots.[19] The kinetic constants of K_M and k_{cat}, the substrate selectivity parameter k_{cat}/K_M, and the rate acceleration (k_{cat}/k_{uncat}) observed for each substrate at pH 8.7 are listed in Table 1. It is worth noting that the K_M values for methionine ester substrates **3** and **4** are approximately 1 order of magnitude higher (more weakly bound antibody–substrate complex) than the K_M values for the norleucine substrates **1** and **2**.

We performed two controls to verify that the observed catalysis was occurring in the combining site of 17E8 and was not a result of an enzyme impurity present in the 17E8 preparation. The first experiment tested hapten **5** for the ability to competitively inhibit the observed 17E8 catalysis. The inhibition analysis was performed by the method of Dixon (data not shown).[12] This analysis showed that the hapten **5** is a competitive inhibitor of 17E8 catalysis (K_i = 500 nM), demonstrating that catalysis is occurring in the 17E8 combining site. In the second control experiment we prepared and purified the Fab fragment of 17E8 and confirmed that the Fab retained the specific activity of hydrolysis observed for the full-length 17E8 immunoglobulin. A sample of 17E8 immunoglobulin was digested with papain, the excess papain was removed by gel filtration chromatography, and the Fab portion of the immunoglobulin was separated from the Fc portion with protein-A affinity chromatography. The 17E8 Fab fragment prepared in this manner was judged to be >95% homogeneous by SDS-PAGE with Coomassie blue staining. In hydrolysis experiments, the Fab material was found to retain the same specific activity of ester hydrolysis as the intact 17E8 IgG.

pH Dependence of 17E8 Catalysis. We examined the pH dependence of 17E8 catalysis with substrates **1–4**. The steady-state kinetics of 17E8-catalyzed hydrolysis with substrates **1–4** were measured at different pH values in the range from 7.2 to 10.5. We were unable to obtain reliable k_{cat} measurements for the two methionine esters **3** and **4** at pH > 10.0, but obtained good data in the pH range 10.0–10.5 for the norleucine esters **1** and **2**. The problem with the methionine esters at elevated pH results from the higher K_M values for these substrates (meaning higher substrate concentrations are required for a k_{cat} determination), combined with the fact that the background reaction is greatly accelerated at pH > 10.0. The k_{cat} values for each substrate are plotted as a function of pH (Figure 2), and the bell-shape of the profiles suggests that catalysis is mediated by two ionizable active site residues. A plot of k_{cat}/K_M vs pH generates a similar bell-shaped profile with similar pK_a values (data not shown), which indicates that the substrate-binding step is not affected in this pH range and that the pK_a's are not significantly perturbed in the Michaelis complex. The antibody displays maximum activity at pH 9.5, which corresponds to a state where one of the antibody ionizable groups is deprotonated and the other is protonated. The pH-rate data for **1–4** gave an excellent fit to a rate equation derived from an equilibrium based on two ionizable groups in the antibody.[20] The pK_a values obtained from this fit varied slightly with the different substrates, but average values of 8.9 ± 0.2 and 10.1 ± 0.2 can be calculated for the first and second ionizable groups, respectively. We believe the rate decrease at pH > 10.0 represents a true ionization event and is not simply a result of antibody denaturation. Support for this position comes from the fact that K_M values for the four substrates do not vary significantly in the pH range 7.2–10.5 and that other laboratories have reported pH-rate studies with catalytic antibodies where the antibody displays maximum activity (k_{cat}) at pH 10.5, indicating that immunoglobulins are stable at this pH.[7,8]

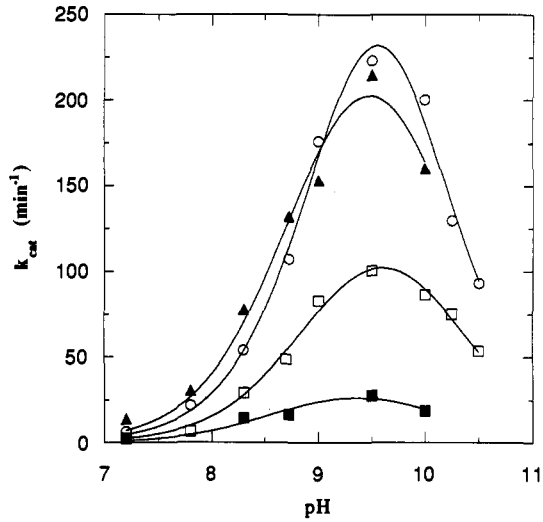

Figure 2. pH-rate profile for 17E8-catalyzed hydrolysis of substrates **1–4**: AcnorleuOPh, **1** (□); fornorleuOPh, **2** (○); AcmetOPh, **3** (■); formetOPh, **4** (▲). Data were fit to a rate equation derived from a scheme based on two ionizable antibody residues.[20] The following pK_a values and correlation coefficients for each substrate were calculated from the fit: **1**, pK_a1 = 8.93 ± 0.07, pK_a2 = 10.27 ± 0.08, R = 0.9953; **2**, pK_a1 = 9.11 ± 0.08, pK_a2 = 9.99 ± 0.08, R = 0.9950; **3**, pK_a1 = 8.6 ± 0.3, pK_a2 = 10.1 ± 0.4, R = 0.9629; **4**, pK_a1 = 8.8 ± 0.2, pK_a2 = 10.2 ± 0.2, R = 0.9915.

Hydroxylamine Partitioning Studies. Hydroxylamine partitioning studies were conducted to determine whether an acyl–antibody intermediate is formed in the 17E8-catalyzed hydrolysis

(19) Segel, I. H. In *Enzyme Kinetics*; Wiley Interscience: New York, 1975; pp 59–61.

(20) The equation used to fit the pH-rate data in Figure 2 was derived from the following scheme:

$$IgH_2 \overset{K_a1}{\rightleftharpoons} IgH \overset{K_a2}{\rightleftharpoons} Ig$$

where the singly ionized form of the antibody, IgH, represents the active form, and K_a1 and K_a2 represent the two equilibrium constants for ionization. Assuming neglible activity in the other two ionization forms IgH_2 and Ig, the following rate equation can be derived:

$$k_{cat(app)} = k_0/(10^{pK_a1-pH} + 1 + 10^{pH-pK_a2})$$

where $k_{cat(app)}$ = the observed k_{cat}, k_o = the maximum k_{cat} achieved if all of the antibody is in the active (IgH) form, and pK_a1 and pK_a2 are the first (low pH) and second (high pH) pK_a values of the antibody ionizable groups, respectively. The pH-rate data for each of the substrates (**1–4**) were fit to this equation using the Kaliedagraph plotting program.

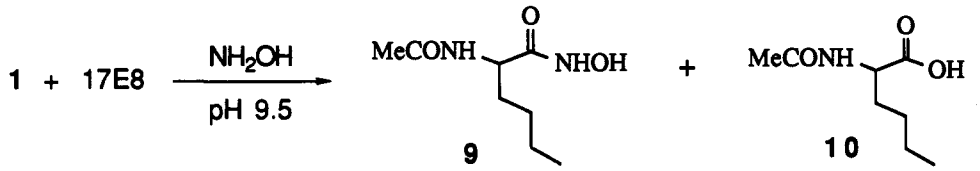

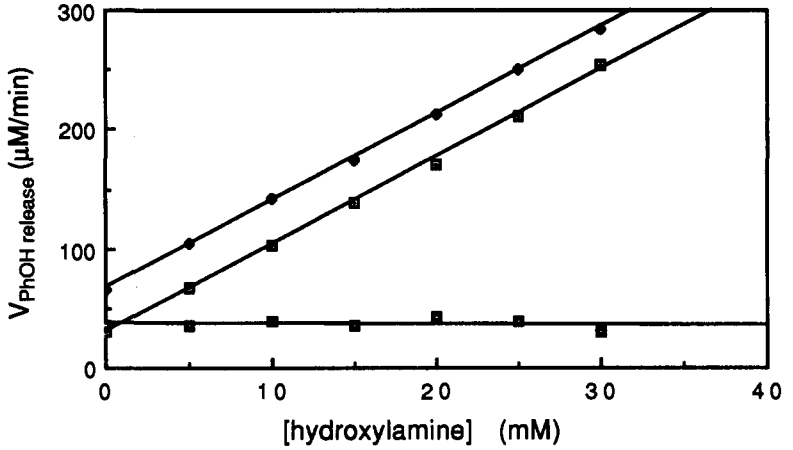

Figure 3. Hydroxylamine partitioning of ester **1** to hydroxamate **9** and carboxylate **10** catalyzed by 17E8. Velocity determinations were made by measuring phenol release (270 nm) using 1.0 mM ester **1** with 0.91 μM 17E8 (pH 9.5) in the presence of hydroxylamine (0–30 mM): antibody-catalyzed rate (◆), uncatalyzed background rate (□), antibody catalyzed rate – uncatalyzed rate (■).

reaction. In the presence of hydroxylamine, an acyl–ester intermediate can partition to give both carboxylic acid and hydroxamic acid products.[21] Hydroxylamine partitioning has been used to probe for serine protease acyl–enzyme intermediate formation with ester and amide substrates and to determine whether intermediate formation or breakdown is the rate-limiting step in catalysis.[13,22,23] We conducted antibody-catalyzed hydroxylamine partitioning experiments that were analogous to the classical enzyme studies, and our objectives were to determine whether an intermediate is formed in the antibody-catalyzed reaction and whether formation or breakdown of the intermediate is the rate-limiting step in catalysis.

The norleucine phenyl ester **1** was used as a substrate in these experiments at V_{max} concentration and at pH 9.5, where 17E8 is most active. The rate of phenol release in the uncatalyzed background reaction is increased significantly in the presence of hydroxylamine (Figure 3). Antibody-catalyzed phenol release in the presence of hydroxylamine, however, proceeds at a rate that is faster than the uncatalyzed reaction. Plots of the antibody-catalyzed and buffer-catalyzed rates of phenol release as a function of hydroxylamine concentration give parallel lines (Figure 3), indicating that the net rate of antibody-catalyzed phenol release from ester **1** is not affected by hydroxylamine concentration.

The identity of hydroxamic acid **9** was confirmed by preparative scale antibody-catalyzed hydroxaminolysis, followed by purification (HPLC) and characterization of **9** by ^{1}H NMR and mass spectrometry. As is the case with other hydroxamic acids, **9** forms a stable complex with ferric chloride that has a characteristic absorbance maximum at 520 nm. This provides a sensitive assay to both identify and quantitate the formation of hydroxamic acid **9**. Using this assay, we found that the 17E8-catalyzed hydroxaminolysis:hydrolysis product ratio (**9**/**9**+**10**) increases with increasing hydroxylamine concentration (Table 2). The buffer-catalyzed hydroxaminolysis:hydrolysis product ratio increases with hydroxylamine to a lesser extent than the antibody-catalyzed partitioning reaction (Table 2). The combined results of the hydroxylamine partitioning experiments summarized in Figure 3 and Table 2 show that a covalent acyl intermediate is formed in 17E8-catalyzed ester hydrolysis and that the formation of this intermediate is the rate-limiting step in 17E8 catalysis.

Table 2. 17E8-Catalyzed Hydroxylamine Partitioning[a]

[NH_2OH] (mM)	17E8-catalyzed **9**/**9**+**10**	buffer-catalyzed **9**/**9**+**10**
0	0	0
10	0.45	0.32
20	0.58	0.38
30	0.67	0.38

[a] Quantitation of **9** was performed by measuring the absorbance of the **9**–ferric chloride complex at 520 nm. Quantitation of **9**+**10** was performed by measuring phenol absorbance at 270 nm.

17E8 Sequence Analysis. The light- and heavy-chain Fab genes of 17E8 were cloned and sequenced using standard procedures.[24] The VJ and VDJ polypeptide sequences of 17E8 deduced from the nucleotide sequences are shown in Figure 4. The heavy-chain constant region sequence (C_H1) of 17E8 was found to be identical with other murine IgG_{2b} sequences, and the light-chain constant region sequence was found to be identical to other murine C_κ sequences.[25]

Discussion

Compared to other reports of catalytic antibodies with esterase activity, 17E8 is among the best catalyts generated to date.[3] At maximum activity (pH 9.5) 17E8 catalyzes the hydrolysis of the *N*-formyl norleucine phenyl ester **2** with k_{cat} = 223 min^{-1} and the *N*-formyl methionine phenyl ester **4** with k_{cat} = 214 min^{-1}. There are two reported examples of antibody-catalyzed ester hydrolyses that proceed at a faster rate than the 17E8-catalyzed reaction, but both of these antibodies are specific for activated phenyl ester substrates.[9,26] The largest rate acceleration (k_{cat}/k_{uncat})

(21) Jencks, W. P. *Catalysis in Chemistry and Enzymology*; McGraw-Hill: New York, 1969; p 228.
(22) Caplow, M.; Jencks, W. P. *J. Biol. Chem.* **1963**, *238*, PC1907–9.
(23) Epand, R. M.; Wilson, I. B. *J. Biol. Chem.* **1963**, *238*, 1718–23.
(24) Sambrook, J.; Fritsch, E. F.; Maniatis, T. *Molecular Cloning: A Laboratory Manual*, 2nd ed.; Cold Springs Harbor Laboratory: Cold Springs Harbor, NY, 1989.
(25) Kabat, E. A.; Wu, T. T.; Perry, H. M.; Gottesman, K. S.; Foeller, C. *Sequences of proteins of immunological interest*, 5th ed.; U. S. Department of Health and Human Services: Washinton, DC, 1991.

A. 17E8 Heavy chain VDJ Sequence

EVQLQESGTELVKPGASVKISCKASGYIFT<u>DHAIH</u>W

VKQRPEQGLEWIG<u>YISPGNGDIKYNEKFKV</u>KATLT

ADKSSSTAYMQLNSLTSEDSAVYFCKR<u>SYYGSSYV</u>

<u>DY</u>WGQGTTLTVSS

B. 17E8 Light Chain VJ Sequence

DIELTQSPSSLSASLGGKVTITC<u>KASQDIKKYIG</u>WY

QHKPGKGPRLLIHY<u>TSTLLP</u>GIPSRFRGSGSGRDY

SFSISNLEPEDIATYYC<u>LQYYNLRT</u>FGGGTKLE

Figure 4. Protein sequence (deduced from DNA sequence) of the heavy-chain variable region (A) and light-chain variable region (B) of 17E8. The C_H1 (IgG_{2b}) and C_κ sequences were identical to other reported murine constant region sequences.[25]

that we measured for the 17E8-catalyzed hydrolysis was 2.2×10^4 obtained with the *N*-formyl methionine substrate **4** at pH 7.2. This is not the optimum pH for the antibody-catalyzed reaction (k_{cat} = 13.4 min^{-1} at pH 7.2), but the background reaction is much slower at pH 7.2 than at 9.5 ($k_{uncat} = 6.2 \times 10^{-4}$ min^{-1} at pH 7.2 vs 4.2×10^{-2} min^{-1} at pH 9.5), which accounts for the larger rate acceleration at pH 7.2.

Product inhibition is a common problem with catalytic antibodies.[3] We did not observe any product inhibition in kinetics experiments with 17E8. Some product inhibition was observed, however, in antibody-catalyzed hydrolysis reactions that were run to greater conversion, resulting in higher product concentrations. We confirmed that phenol is the inhibitory product and that inhibition occurs with the buildup of approximately 300 μM phenol (data not shown). This weak product inhibition did not affect any of our kinetic and mechanistic experiments that measure initial rates. Moreover, because of the high level of activity of 17E8, sub-micromolar antibody concentrations can be employed, and under these conditions more than 1000 catalytic turnovers can be measured before any product inhibition occurs.

Because we examined the hydrolysis of a series of closely related amino acid esters, side-chain and *N*-acyl group structure–activity relations for 17E8 catalysis are evident from the data shown in Table 1. The two *N*-formyl substrates (**2** and **4**) give higher k_{cat} and K_M values compared to the *N*-acetyl substrates (**1** and **3**). Comparing the substrate selectivity parameters (k_{cat}/K_M) shows that both the *N*-formyl esters are better substrates for 17E8 than the corresponding *N*-acetyl esters. This effect is interesting because the phosphonate **5** used to elicit 17E8 contains a methylene unit at this position, which is more structurally similar to the acetyl methyl group than the formyl hydrogen. It therefore appears that the better substrate for 17E8 catalysis is the one which is structurally more dissimilar at this position to the antigen, and this effect is worth a factor of 2 (**4** vs **3**) in k_{cat}/K_M. The effect is more prevalent at V_{max} conditions, where the observed rate acceleration (k_{cat}/k_{uncat}) for the *N*-formyl methionine substrate (**4**) is 6-fold larger than that of the *N*-acetyl methionine substrate (**3**).

Amino acid side-chain selectivity can be seen by comparing the k_{cat}/K_M values for the norleucine esters (**1** and **2**) with the methionine esters (**3** and **4**). The *N*-acetyl norleucine ester (**1**) is a better substrate for 17E8 than the *N*-acetyl methionine ester (**3**) by a factor of 8 in k_{cat}/K_M, and a similar trend is seen in the *N*-formyl series, where the k_{cat}/K_M for norleucine ester **2** is a factor of 6 higher than that of the methionine ester **4**. Hapten **5** contains the norleucine amino acid side chain, and the only difference in these two sets of substrates (**1**, **2** vs **3**, **4**) is the replacement of the third side-chain methylene unit with a sulfur atom. This analysis of side-chain selectivity contrasts the above amino-substituent results and shows that ester substrates containing the same amino acid side chain as the hapten **5** are better substrates for 17E8. Under V_{max} conditions this side-chain effect is evident for the *N*-acetyl substrates (**1** vs **3**), but is less pronounced for the *N*-formyl substrates because the observed rate acceleration for both **2** and **4** is approximately 10^4.

There is a distinct bell-shaped pH dependence for each of the four amino acid ester substrates, which is consistent with a mechanism involving two ionizable groups in the antibody (Figure 2). The maximum activity for 17E8 is achieved at pH 9.5, and k_{cat} for the *N*-formyl norleucine ester **2** at this pH is a factor of 34 greater than the k_{cat} obtained with **2** at pH 7.2. In the active state of 17E8, one of the ionizable groups is protonated and the other is deprotonated. The calculated pK_a's for these two groups are 10.1 and 8.9, respectively.

The phosphonate hapten **5** contains an oxyanion that mimics the developing oxyanion in the rate-limiting transition state of ester hydrolysis. The pK_a 10.1 group falls in the range of a lysine residue, and the fact that the observed catalysis substantially decreases for each of the four substrates at pH > 10 supports the idea that this residue functions in catalysis by stabilizing oxyanion development. The 17E8 variable region sequence shows that there are three lysine residues in CDR2 of the heavy chain and three lysine residues in CDR1 of the light chain (Figure 4).

The pK_a 8.9 group is an acidic residue that accelerates hydrolysis in its deprotonated state. This behavior suggests that this residue functions either as a nucleophile or as a general base to enhance the nucleophilicity of water or another side-chain functional group such as a serine hydroxyl. Potential candidates for this residue include a cysteine thiol (pK_a range in proteins 8–11) and a tyrosine hydroxyl (pK_a range in proteins 9–12).[4] Cysteine can be ruled out because the only cysteine residues present in the 17E8 sequence are the conserved framework residues that exist as disulfide bonds in all antibodies (Figure 4).[25] Several tyrosine residues are present, however, in the CDRs of both the heavy and light chain.

In hydrolysis experiments with 17E8 and ester **1** conducted in the presence of hydroxylamine, both amino acid and aminohydroxamic acid products are formed (Figure 3, Table 2). These results are consistent with a catalytic mechanism involving the formation of a covalent acyl intermediate, shown in Figure 5A. Covalent acyl–antibody species have been proposed as intermediates for other acyl-transfer catalytic antibodies.[7,8,26] In the case of 17E8, the fact that the velocity of hydrolysis/hydroxaminolysis as measured by phenol release is unaffected by hydroxylamine concentration while the ratio of **9**:**10** increases with increasing hydroxylamine suggests that formation of the acyl intermediate is the rate-determining step in 17E8-catalyzed hydrolysis.[21] Similar hydroxylamine partitioning is observed with serine proteases such as chymotrypsin, which catalyze the hydrolysis of ester and amide substrates through the formation of a common acyl–enzyme intermediate.[27] With chymotrypsin, acyl–enzyme formation is generally the rate-limiting step with amide substrates, and acyl–enzyme breakdown is rate-limiting with ester substrates.

Our data suggest that a covalent acyl intermediate forms in the active site of 17E8 (Figure 5B) either through the direct participation of a nucleophilic tyrosine residue or *via* a kinetically equivalent mechanism where an ionized tyrosine enhances the nucleophilicity of a neighboring residue (such as a serine) through general base catalysis. A second possibility is that the acyl intermediate is an oxazolone that is formed through a cyclization

(26) Gibbs, R. A.; Benkovic, P. A.; Janda, K. D.; Lerner, R. A.; Benkovic, S. J. *J. Am. Chem. Soc.* **1992**, *114*, 3528–34.

(27) Walsh, C. *Enzymatic Reaction Mechanisms*; Freeman: San Fransisco, 1979; pp 53–97.

A. Mechanistic Scheme for Hydrolysis/Hydoxaminolysis

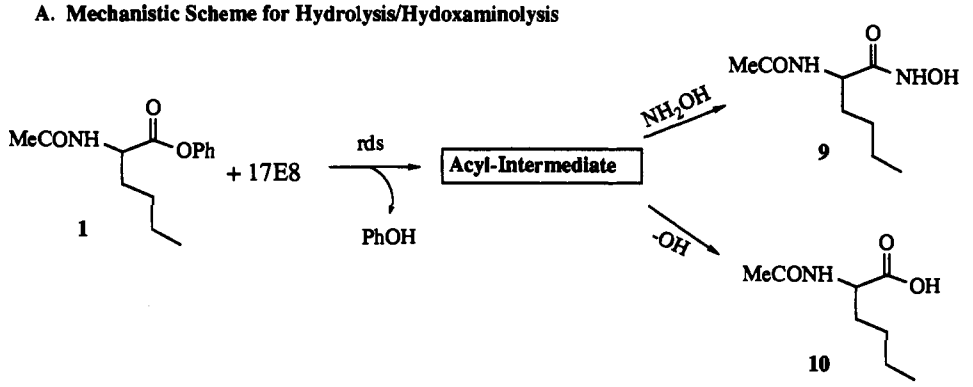

B. Possible Acyl-Intermediates

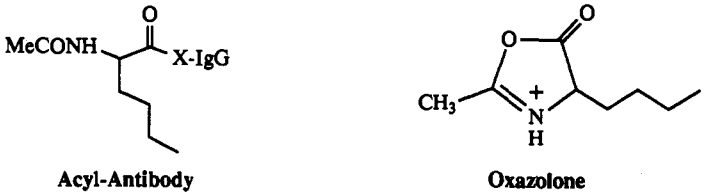

Acyl-Antibody **Oxazolone**

Figure 5. Mechanistic implications of kinetic and hydroxylamine partitioning experiments. (A) The data in Figure 3 and Table 2 support a mechanism involving the formation of an acyl intermediate where intermediate formation is the rate-determining step (rds) in the catalyzed reaction. (B) Possible structures for the acyl intermediate include a covalently bound acyl–antibody species or a noncovalently bound oxazolone species.

mechanism involving the substrate *N*-acyl group (Figure 5B). This intermediate would not be covalently bound to the antibody active site, but its formation would have to be catalyzed by the ionization of the pK_a 8.9 residue. A deeper understanding of the unique active site chemistry and mechanism of action of 17E8 will come from three-dimensional structure determination of the antibody–hapten complex. We have grown crystals of the 17E8 Fab-**5** complex and collected X-ray diffraction data at 2.5-Å resolution.[28] The three-dimensional structure of this catalytic antibody transition-state analog complex will be reported elsewhere.

Although a phosphonate transition-state analog was used to elicit 17E8, our results indicate that more is involved with the hydrolytic mechanism than simple transition state stabilization. As has been noted for other phosphonate-derived catalytic antibodies,[7b] acyl intermediate formation in our system was not deliberately programmed from hapten design, but is instead a fortuitous result of immunoglobulin variable region diversity. An understanding of the 17E8 catalytic mechanism from a structure/function standpoint could lead to the generation of mutants with higher levels of catalytic activity. More active mutants could be generated in a structure-guided approach by site-directed mutagenesis or using random mutagenesis coupled to a methionine-dependent functional selection.[15,17] These studies could help define the limits of catalytic activity that can be incorporated into antibody molecules and could also shed light on the pathways of enzyme evolution.

(28) Zhou, G. W.; Gou, J.; Huang, W.; Fletterick, R. J.; Scanlan, T. S. Unpublished results.

Acknowledgment. This work was supported by Research Grant BE-140 from the American Cancer Society. Mass spectral analysis of synthetic compounds was provided by the UCSF Mass Spectrometry Facility (A. L. Burlingame, Director) supported by the Biomedical Research Technology Program of the National Center for Research Resources, NIH NCRR BRTP 01614, and NIH NIEHS ES04705. We gratefully acknowledge Kevan Shokat, Jim Stephens, Jeff Jacobs, Neil Buckley, and Phyllis Kosen for helpful discussions.